



HAL
open science

UHF-RFID Read Range Characterization Method Using Power Activation Profiles

Hadi El Hajj Chehade, Bernard Uguen, Sylvain Collardey

► **To cite this version:**

Hadi El Hajj Chehade, Bernard Uguen, Sylvain Collardey. UHF-RFID Read Range Characterization Method Using Power Activation Profiles. *Ieee Journal of Radio Frequency Identification*, 2023, 7, pp.134-144. 10.1109/JRFID.2023.3277313 . hal-04148939

HAL Id: hal-04148939

<https://hal.science/hal-04148939>

Submitted on 5 Jul 2023

HAL is a multi-disciplinary open access archive for the deposit and dissemination of scientific research documents, whether they are published or not. The documents may come from teaching and research institutions in France or abroad, or from public or private research centers.

L'archive ouverte pluridisciplinaire **HAL**, est destinée au dépôt et à la diffusion de documents scientifiques de niveau recherche, publiés ou non, émanant des établissements d'enseignement et de recherche français ou étrangers, des laboratoires publics ou privés.



Distributed under a Creative Commons Attribution - NonCommercial 4.0 International License

UHF-RFID Read Range Characterization Method Using Power Activation Profiles

Hadi El Hajj Chehade, Bernard Uguen, *Member, IEEE*, Sylvain Collardey, *Member, IEEE*

Abstract—This paper presents a detailed characterization of passive UHF-RFID tags using measured power activation profiles. Factors such as chip sensitivity, antenna dimension, and conjugate impedance matching are taken into account. Results are presented in a proposed chart relating the square root of the modulation factor to the mean power transmission coefficient, providing a fine-grained comparison of tag performance. The free space read range of tags is then investigated as a function of mean transmission coefficient, modulation factor, chip and reader sensitivity. The approach is illustrated and validated through a measurement campaign on a set of 9 commercial tags. The proposed characterization procedure enables an accurate assessment of tag performance.

Index Terms—UHF-RFID, RFID tag characterization, Chip sensitivity, RFID power profiles, Read range, Multipath, Channel reciprocity.

I. INTRODUCTION

RADIO-frequency identification (RFID) has become an integral part of supply chain management, inventory control, and asset tracking in various industries. UHF RFID tags are widely used in these applications due to their ability to operate over long distances and the ability to read multiple tags simultaneously. Tag characterization is an important task to evaluate the efficiency and reliability of RFID systems. In this paper, we present a novel UHF RFID tag characterization method which is independent from the environment and give access to intrinsic properties of the tag by using a simple measurement setup.

Passive tags use backscatter modulation to communicate with a reader. The tag's antenna captures electromagnetic power to feed the transponder chip. When the minimum required power is fed to the tag's chip, it activates, it demodulates the commands received from the reader, and modulates them back with a portion of the absorbed energy [1], [2]. The chip sensitivity is an intrinsic characteristic which represents the minimum required power for a chip to be activated. It is shown in [3] that the antenna size has also a great impact on performance.

RFID tags must be rigorously characterized, which is a challenging task. An important aspect of RFID characterization is the read range, which is the most widely used and practical performance indicator. Its evaluation relies on a free space assumption, the read range is obtained indirectly based on the Friis formula, without necessarily measuring the tag at its limit distance [4], [5]. More recently, we have also seen

works that exploit different variations of parameters over the air in order to characterize RFID tags based on frequency variation [6], angular variation [7], and distance variation [8]. The principle of varying jointly distance and transmitted power has been demonstrated to be very fruitful in order to access tag characteristics. It is based on estimating the minimum power required to energize the tags at a fixed controllable distance [9], [10]. This is also the approach chosen in this paper. We present a theoretical approach to characterize the tag over-the-air, and which is validated experimentally. However, the method presented in this paper is independent from the channel and doesn't require a previous knowledge of gains and losses that are occurring in the RFID system, since it is not based on the Friis equation, but rather on the channel reciprocity. We show how the acquisition of the power profiles over a controllable distance can be exploited to characterize, evaluate and compare the tag performance. Therefore, the proposed method requires only a tag, a reader and a setup to control the distance between the tag and the reader.

In this paper, we use an experimental process based on incident power variation and distance (or angular) variation to access a meaningful quantity related to the chip sensitivity called tag receptivity. This design dependent parameter is then identified and discussed over different examples.

The theoretical aspects in section II aims to describe key concepts related to RFID tag characterization. We start by addressing power transmission aspects, by describing the power transmission coefficient τ and the modulation factor M . We also define the received power activation profile and the transmitted power activation profile, which allow to measure the effectiveness of power transmission. Next, we introduce a Q^{th} factor obtained from the defined profiles and explain its relation to tag receptivity. We propose a convenient (\sqrt{M}, τ) chart where a tag can be placed and its performance evaluated, and then compared with other tags. For that purpose, an interval halving algorithm is proposed in order to place on the chart a set of tags measured in the same conditions. This requires to also measure the ratio between their respective power transmission coefficients. We finish this section by providing an expression for the read range under the assumption of free space propagation.

In section III, we take a closer look at the new proposed chart for evaluating UHF RFID tags formed by combining known chips and antennas presented originally in [11]. We illustrate how the proposed chart can be used to make informed decisions when choosing tag for an application. The proposed chart allows easy ranking of UHF RFID tag formed by a set of combination chip-antenna.

The authors are with *Univ Rennes, CNRS, IETR - UMR 6164*, F-35000, Rennes, France (e-mail: {hadi.chehade, bernard.uguen, sylvain.collardey}@univ-rennes.fr).

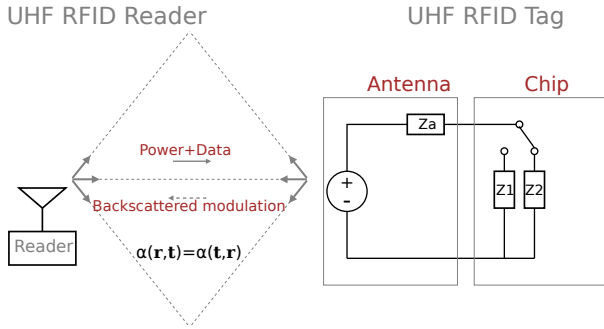


Fig. 1: Principle of an RFID tag activation over a reciprocal channel

In section IV, we cover various aspects of UHF RFID tag performance evaluation. Firstly, we describe the experimental setup used in the evaluations. Secondly, we present the measured power profiles of the tags under evaluation. Following this, we compare a set of commercial tags using their measured power-distance profiles. Then we evaluate the distribution of the extracted tag receptivity error. To make a thoughtful evaluation, we provide an illustrated comparison of the tags using the proposed chart. Finally, we present an example of ranking of tag performances, based on various indicator including free space read range, facilitating the choice of the appropriate tag for a given application.

II. THEORETICAL ASPECTS

A. Mean Power Transmission Coefficient

The RFID tag operation consists of absorbing and back-scattering the energy received from a reader. Let consider a RFID chip has two impedance states : Z_1 a low state impedance (typically a short circuit) and Z_2 a high state impedance as shown in Fig. 1 and detailed in [1]. For the sake of simplicity, the author [11] assumes that the low state impedance is a short circuit ($Z_1 = 0$) while it is shown in [12], [13] that practically this impedance is not strictly zero and may vary with respect to (w.r.t) the applied power. Generally, the complex conjugate matching condition $Z_a^* = Z_2$ is enforced by design to maximize the power transfer whatever the value of Z_1 which is not provided in the datasheet. Note that in [14] and [11], the power transmission coefficient τ depends only on the input state Z_2 . However, the τ defined in this work considers the absorption in both states.

When an incident wave with a power density S (measured in W/m^2) hits an RFID tag, the tag absorbs a portion of the energy and reflects the rest in all directions. The proportion of the energy that is backscattered towards the RFID reader depends on the tag's gain in the reader's direction. This gain also determines the amount of energy absorbed by the tag. The tag's effective surface area (expressed in m^2) is related to its gain (G_t) and the wavelength ($\lambda = \frac{c}{f}$ where c is the speed of light) of the incident wave:

$$A_e = \frac{G_t \lambda^2}{4\pi} \quad (1)$$

The effective surface A_e allows to express the quantity of power taken from the incident field. But as it is a question of communicating information with the reader, the tag cannot be permanently in the absorption mode, it must also dedicate itself portions of time with less absorption and more back-scattering. What matters for the receiver is the power of the fluctuation between these two states 1 and 2, the dynamic power carried by the modulation of the signal. But as this fluctuation is generated by an energy previously captured by the tag, the energy balance necessarily involves a memory effect and must result from an integrating over time. On average, the energy received by the tag must be divided equally between the energy used to power the tag and the energy statically and dynamically backscattered to the environment. Only the energy of the side bands of the spectrum is exploitable in reception for the demodulation. The total electromagnetic power available at the tag is therefore $P_r = SA_e$ expressed in Watts. This total power is decomposed into a term absorbed by the device and a term back-scattered to the environment:

$$\underbrace{SA_e}_{total} = \underbrace{SA_e(1 - |\Gamma_i|^2)}_{absorbed} + \underbrace{SA_e|\Gamma_i|^2}_{reflected} \quad (2)$$

$$\underbrace{SA_e}_{total} = \underbrace{SA_e\tau_i}_{absorbed} + \underbrace{SA_e|\Gamma_i|^2}_{reflected} \quad (3)$$

Where we introduce, the complex reflection coefficient:

$$\Gamma_i = \frac{Z_i - Z_a^*}{Z_i + Z_a} \quad (4)$$

and the τ_i parameter introduced in [14]. In this paper, we introduce the distinction between the power transmission coefficient:

$$\tau_i = 1 - |\Gamma_i|^2 \quad (5)$$

and the mean power transmission coefficient over both states (assuming the same time on both states) :

$$\tau = \frac{\tau_1 + \tau_2}{2} = 1 - \frac{|\Gamma_1|^2 + |\Gamma_2|^2}{2} \quad (6)$$

τ refers to the mean of the absorption over the two switched impedance unlike in [14], [11].

B. Modulation Factor

The RFID principle consists on switching the termination load, thereby modulating the reflecting coefficient of the tag. Assuming a modulation with a shaping function g , a symbol duration T and $\Gamma_k \in [\Gamma_1, \Gamma_2]$ associated to an equiprobable binary train of symbols, we can express the dynamic reflecting coefficient as follows:

$$\Gamma(t) = \sum_{k \in \mathbb{Z}^+} \Gamma_k g(t - kT) \quad (7)$$

Assuming that the two commutated states are equiprobable, we obtain the expected value of the reflecting coefficient as:

$$E[\Gamma_k] = \frac{\Gamma_1 + \Gamma_2}{2} \quad (8)$$

In [15], the authors introduce the idea of separation between a static and a dynamic contribution, obtained in centering the modulated signal around its mean value. This can be simply written as:

$$\Gamma(t) = \underbrace{E[\Gamma_k]}_{\Gamma_s} + \underbrace{\sum_k (\Gamma_k - E[\Gamma_k])g(t - kT)}_{\Gamma_d(t)} \quad (9)$$

Where a static Γ_s and a dynamic $\Gamma_d(t)$ term have been exhibited. If we now consider the expectation of the square modulus of this quantity, assuming the ergodicity of the signal, it yields

$$E(|\Gamma(t)|^2) = |\Gamma_s|^2 + E(|\Gamma_d(t)|^2) \quad (10)$$

The second term of the right hand side is called the modulation factor M in [14].

$$M = E(|\Gamma_d(t)|^2) = \frac{|\Gamma_1 - \Gamma_2|^2}{4} \quad (11)$$

By introducing (8) and (11) in (10) we obtain

$$E(|\Gamma(t)|^2) = \frac{|\Gamma_1 + \Gamma_2|^2}{4} + \frac{|\Gamma_1 - \Gamma_2|^2}{4} = \frac{|\Gamma_1|^2 + |\Gamma_2|^2}{2} \quad (12)$$

Or equivalently,

$$\underbrace{\frac{|\Gamma_1 + \Gamma_2|^2}{4}}_{static} + \underbrace{M}_{dynamic} = \underbrace{1 - \tau}_{scattered} \quad (13)$$

The static term is responsible for the power of the waveform carrier while the dynamic term, which is also the useful term for the tag detection, is responsible for the power in the sidelobes of the modulated spectrum. This relation is simply expressing the energy conservation over time.

C. Particularization of the Channel Coefficient in Free Space

As the impinging power is not directly accessible, in the following we replace the dependency with P_{inc} with the double dependency with P_t and spatial information of reader and tag \mathbf{r} and \mathbf{t} . Where $\mathbf{r} = [\vec{p}_r, \theta_r, \phi_r]$ and $\mathbf{t} = [\vec{p}_t, \theta_t, \phi_t]$ are 5 dimensional vectors gathering position and orientation of reader and tag.

The joint effect of the transmission channel including the tag and reader antenna is expressed in the channel coefficient $\alpha(f, \mathbf{r}, \mathbf{t})$. This is a scalar quantity which account for the channel reciprocity because \mathbf{r} and \mathbf{t} are commuting variables meaning this term is the same for the forward and backward link.

$$\alpha(f, \mathbf{r}, \mathbf{t}) = \int_{\Omega_r \times \Omega_t} G_r(f, \Omega_r) C G_t(f, \Omega_t) d\Omega_t d\Omega_r \quad (14)$$

Where $C \equiv C(f, \vec{p}_r, \Omega_r, \vec{p}_t, \Omega_t)$ is the power transfer function of the channel, which depends on the position and orientation of both the reader and the tag. For a free space channel we would have the simplification:

$$C(\vec{p}_r, \Omega_r, \vec{p}_t, \Omega_t) = \frac{\delta(\Omega_r - \omega_r) \delta(\Omega_t - \omega_t)}{4\pi |\vec{p}_r - \vec{p}_t|^2} \quad (15)$$

where $\omega_r = (\theta_r, \phi_r)$, $\omega_t = (\theta_t, \phi_t)$ and $d = |\vec{p}_r - \vec{p}_t|$ such that

$$\alpha_{FS}(f, \mathbf{r}, \mathbf{t}) = \frac{G_r(f, \omega_r) G_t(f, \omega_t)}{4\pi d^2} \quad (16)$$

We define $P_{inc}(P_t, f, \mathbf{r}, \mathbf{t})$ as the incident power on the tag at a configuration \mathbf{t} from the reader at configuration \mathbf{r} .

$$P_{inc}(P_t, f, \mathbf{r}, \mathbf{t}) = P_t \alpha(f, \mathbf{r}, \mathbf{t}) \frac{\lambda^2}{4\pi} \quad (17)$$

The multipath fading and the polarization factor is assumed to be all included in the α term which is a deterministic non linear function of positions, antennas orientation and frequency f . In the basic free space situation we recover the well known expression

$$P_{inc}(P_t, f, d) = P_t G_t G_r \left(\frac{\lambda}{4\pi d} \right)^2 \quad (18)$$

D. Definition of the Transmitted Activation Profile

In average on the two commutated states, a fraction P_{IC} of this power is absorbed by the tag Integrated Circuit (IC), neglecting the losses.

$$P_{IC}(P_t, f, \mathbf{r}, \mathbf{t}) = P_{inc}(P_t, f, \mathbf{r}, \mathbf{t}) \tau(P_t, f, \mathbf{r}, \mathbf{t}) \quad (19)$$

Where $\tau(P_t, f, \mathbf{r}, \mathbf{t})$ is the previously defined mean power transmission coefficient. Let S_c be the reading power sensitivity threshold of the chip which is an information provided by the chip manufacturer. The activation power $P_t^{th}(f, \mathbf{r}, \mathbf{t})$ corresponds to the transmit power required to reach the IC chip sensitivity:

$$P_{IC}(P_t^{th}, f, \mathbf{r}, \mathbf{t}) = S_c \quad (20)$$

This equality determines the transmitted activation profile $P_t^{th}(f, \mathbf{r}, \mathbf{t})$ which corresponds to the transmit power required to activate the tag at a given position. By using the simplified expression

$$\tau^{th} = \tau(P_t^{th}, f, \mathbf{r}, \mathbf{t})$$

it yields :

$$P_t^{th}(f, \mathbf{r}, \mathbf{t}) = \frac{4\pi S_c}{\lambda^2 \alpha(f, \mathbf{r}, \mathbf{t}) \tau^{th}} \quad (21)$$

This simply means that the tag activates when the impinging power reaches the IC threshold S_c . This profile can be easily characterized by sweeping the transmission power of the reader for each position of the tag.

E. Definition of the Received Power Activation Profile

We define the received power profile $P_r(P_t, f, \mathbf{r}, \mathbf{t})$ which involves twice the reciprocal propagation channel due to forward and backward propagation as:

$$P_r(P_t, f, \mathbf{r}, \mathbf{t}) = P_{inc} M(P_t, f, \mathbf{r}, \mathbf{t}) \alpha(f, \mathbf{r}, \mathbf{t}) \frac{\lambda^2}{4\pi} \quad (22)$$

$$P_r(P_t, f, \mathbf{r}, \mathbf{t}) = \frac{P_t \lambda^4}{(4\pi)^2} \alpha^2(f, \mathbf{r}, \mathbf{t}) M(P_t, f, \mathbf{r}, \mathbf{t}) \quad (23)$$

By considering $P_t = P_t^{th}(f, \mathbf{r}, \mathbf{t})$, we obtain the received power at the activation transmitted power which is noted as the received power activation profile:

$$P_r^{th}(f, \mathbf{r}, \mathbf{t}) = \frac{P_t^{th}(f, \mathbf{r}, \mathbf{t}) \lambda^4}{(4\pi)^2} \alpha^2(f, \mathbf{r}, \mathbf{t}) M^{th} \quad (24)$$

Where $M^{th} = M(P_t^{th}, f, \mathbf{r}, \mathbf{t})$

Hereafter for concision, the explicit parameter dependencies are omitted.

F. Definition of the Tag receptivity R_t^{th} and the Q^{th} factor

By expressing the channel coefficient from (21) we get

$$\alpha = \frac{4\pi S_c}{P_t^{th} \lambda^2 \tau^{th}} \quad (25)$$

In introducing this expression in (23), it simplifies into a relation independent of the transmission channel.

$$P_r P_t^{th2} = P_t S_c^2 \frac{M}{\tau^{th2}} \quad (26)$$

or equivalently:

$$R_t = \frac{\sqrt{M}}{\tau^{th}} S_c = \sqrt{\frac{P_r P_t^{th2}}{P_t}} \quad (27)$$

If we particularize this expression at the activation power $P_t = P_t^{th}$, it becomes:

$$R_t^{th} = Q^{th} S_c = \sqrt{P_r^{th} P_t^{th}} \quad (28)$$

R_t^{th} is the chip sensitivity multiplied by the design dependent factor Q^{th} .

$$Q^{th} = \frac{\sqrt{M^{th}}}{\tau^{th}} \quad (29)$$

If we express (28) in dB scale, we get a dB offset which is a combination of the 3 main intrinsic properties of the tag: $S_{c,dB}$, τ^{th} and M^{th} . The typical chip sensitivity S_c can be obtained from the tag IC datasheet.

$$R_{t,dB}^{th} = 5 \log_{10} M^{th} - 10 \log_{10} \tau^{th} + S_{c,dB} \quad (30)$$

A practical relation is obtained from the right hand side of (27) which gives access to the tag receptivity simply in averaging the transmitted activation profile and the associated received activation profile.

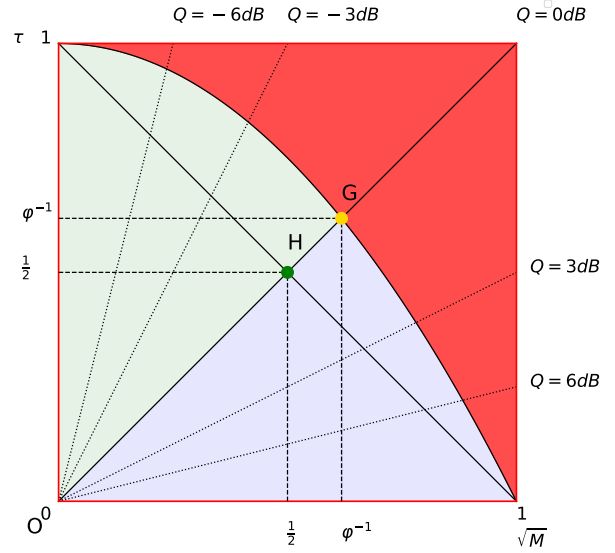


Fig. 2: The proposed (\sqrt{M}, τ) chart

$$R_{t,dB}^{th} = \frac{P_r^{th}_{dB} + P_t^{th}_{dB}}{2} \quad (31)$$

Q_{dB}^{th} is obtained experimentally from the dB offset between the typical chip sensitivity and the above measured tag receptivity as:

$$Q_{dB}^{th} = \bar{R}_{t,dB}^{th} - S_{c,dB} \quad (32)$$

Where $\bar{R}_{t,dB}^{th}$ is the mean value of $R_{t,dB}^{th}$ value. It is observed experimentally that this quantity has a very small variance as shown in section IV-D.

G. Introduction of the (\sqrt{M}, τ) Chart

As we have seen τ accounts for the absorption of the tag and M for its reflectivity or the contrast that is presented to the reader on the return path. An RFID is as good as it provides the proper balance between energy harvesting and high receiving contrast simultaneously. The goal is often to maximize both of these quantities. Given that τ and M are quantities that range from 0 to 1, it is natural to try to find an appropriate representation that can synthesize the performance of an RFID tag for a given frequency and incident power on the tag. Instead of representing τ w.r.t M as it could be envisaged, we propose representing τ w.r.t \sqrt{M} . This has the advantage of facilitating the interpretation of the values of constant Q which are manifested by straight lines originating from the origin. The upper parabolic boundary corresponds to the limit situation where $M = 1 - \tau$, which corresponds, if we return to formula (13), to the situation where the tag does not backscatter any power on the carrier frequency, resulting in maximum power in the sidebands and thus maximizing the contrast M for a given power transmission coefficient τ .

Fig. 2 presents the proposed chart. A tag at a given frequency is a point on this chart at coordinates (\sqrt{M}, τ) .

We have distinguished 3 regions based on the values of \sqrt{M} an τ .

- The red region represents the impossible region for a tag's design.
- The light blue region corresponds to the region where $Q_{dB}^{th} > 0$, therefore $\sqrt{M} > \tau$.
- The light green region corresponds for the region where $Q_{dB}^{th} < 0$, therefore $\sqrt{M} < \tau$.

The upper frontier corresponds also to the condition :

$$|\Gamma_1 + \Gamma_2|^2 = 0$$

i.e the two complex reflecting coefficient symmetrically spaced w.r.t origin.

For a given value of Q we get limitations on the possible values of τ and \sqrt{M} as the intersection between the line of slope Q (expressed in (29)) and the parabolic boundary $M = 1 - \tau$. The resulting limitations are as follows:

$$\tau_{max}(Q) = \frac{\sqrt{1 + 4Q^2} - 1}{2Q^2} \quad (33)$$

$$\sqrt{M_{max}}(Q) = \frac{\sqrt{1 + 4Q^2} - 1}{2Q} \quad (34)$$

If we impose additionally that $\frac{\sqrt{M}}{\tau} = 1$, we obtain $\sqrt{M_{max}} = \varphi^{-1}$ and $\tau_{max} = \varphi^{-1}$ which maximizes simultaneously mean absorption and contrast with the gold number $\varphi = \frac{1+\sqrt{5}}{2}$, $\varphi^{-1} \approx 0.618$. A remarkable point in the chart is then $G = (\varphi^{-1}, \varphi^{-1})$. Notice that if $Z_1 = 0$, then $|\Gamma_1| = 1$ and the best achievable point is $H = (\frac{1}{2}, \frac{1}{2})$, where $\tau_{max} = \frac{1}{2}$.

In the chart, a constant Q corresponds to a line that starts from the origin and has a slope of $\frac{1}{Q}$ since $\tau = \frac{\sqrt{M}}{Q}$.

Furthermore, we define two heuristical criteria to evaluate the tag performance: one is obtained by calculating the Euclidean distance between the point presenting the tag in the chart $T = (\sqrt{M}, \tau)$ and the point G (defined by $\rho_{\varphi^{-1}}$), and the other is obtained by calculating the Euclidean distance between T and H which represents a perfect conjugate matching (defined by $\rho_{\frac{1}{2}}$).

The following equations express the two proposed criteria:

$$\rho_{\varphi^{-1}} = \left(1 - \frac{\|\vec{TG}\|}{\|\vec{OG}\|}\right) \times 100\% \quad (35)$$

$$\rho_{\frac{1}{2}} = \left(1 - \frac{\|\vec{TH}\|}{\|\vec{OH}\|}\right) \times 100\% \quad (36)$$

We assume implicitly that the closer the tag is to either G or H , the better the design. Hence, the higher the values of either $\rho_{\varphi^{-1}}$ or $\rho_{\frac{1}{2}}$, the better the tag performance.

H. Power Transmission Coefficient Ratio between Tags

If we consider two different RFID tags $T_{(i)}$ and $T_{(j)}$ placed at the same position in the same channel (important condition) we have the relation :

$$\frac{P_t^{th_i}(\mathbf{r}, \mathbf{t})}{P_t^{th_j}(\mathbf{r}, \mathbf{t})} = \frac{S_c^{(i)} \tau_j^{th}}{S_c^{(j)} \tau_i^{th}} = \frac{S_c^{(i)}}{S_c^{(j)}} \tau_{i,j} \quad (37)$$

Where $\tau_{i,j}$ is the ratio between two values of mean power transmission coefficient $\tau_{(i)}$ and $\tau_{(j)}$ as:

$$\tau_{i,j} = \frac{\tau_{(j)}}{\tau_{(i)}} \quad (38)$$

it is obtained from the offset between activation profiles of two tags and the ratio of their respective chip sensitivity as:

$$\tau_{i,j} = \frac{P_t^{th_i}(\mathbf{r}, \mathbf{t}) S_c^{(j)}}{P_t^{th_j}(\mathbf{r}, \mathbf{t}) S_c^{(i)}} \quad (39)$$

This measured ratio will be exploited in the next subsection in the attempt of best placing tags on the chart based on the knowledge of their Q^{th} and several $\tau_{i,j}$ ratios.

I. Interval Halving Algorithm to Place Tags in the Chart

In practice, a single tag cannot be placed in the chart from the only knowledge of its Q^{th} factor. Hopefully, if several tags activation profiles are measured and their $\tau_{i,j}$ ratio (offset in dB scale) are evaluated, the task becomes partly achievable. Let assume a set of N tags, placed at the same position, measured in the same channel, and whose profiles are measured under as similar conditions as possible. Let then define the sequence of Q :

$$\mathbf{Q} = [Q_1, \dots, Q_N] \quad (40)$$

and the corresponding sequence of ratio (38) between consecutive values of τ :

$$\mathbf{t} = [\tau_{1,2}, \dots, \tau_{N-1,N}] \quad (41)$$

These two vectors are provided as inputs of the interval halving algorithm (Algorithm 1) which guesses for each tag n its τ_n and $\sqrt{M_n}$ values.

The general principle of the algorithm is the following:

- Each tag should be placed on the line corresponding to its Q value.
- All the ratios involving a tag should be respected. This is obtained iteratively by an interval halving procedure, which adjust the τ value of the first tag until all the tags have their τ less or equal than τ_{max} . This is achieved through cond1.
- The highest value of τ can be optionally limited in a reasonable range defined as τ_{lim} . This is achieved through cond2.

J. Free Space Read Range Formulation

If we assume a free space propagation situation the read range can be constrained either by the forward or the backward link. In the one hand, the read range is a function of τ when limited by the tag activation

$$d_{max}^{(\tau)} = \frac{\lambda}{4\pi} \left(\frac{P_t^{max} G_t G_r \tau}{S_c} \right)^{1/2} \quad (42)$$

On the other hand, in defining the reader sensitivity as S_r , the read range is a function of M when limited by the backward link

Algorithm 1 Determine \sqrt{M}_n and τ_n by interval halving

Require: $\mathbf{Q}, \mathbf{t}, \tau_{lim}, \epsilon$
Output : \sqrt{M}_n and τ_n
 $\tau_{max} = f(\mathbf{Q})$ using eq (33)
 $x_0 = \tau_{max}[0]$
 $x_1 = \tau_{max}[0] + 2\epsilon$
 $k=2$
 $i=1$
while $|x_{i-1} - x_i| > \epsilon$ **do**
 $\mathbf{v} = [x_{i-1}, \mathbf{t}]$
 $\mathbf{pv}[n] = \prod_{i=1}^n \mathbf{v}[i] \quad \forall n \in \{1, \dots, N\}$
 $\text{cond1} = \exists(\mathbf{pv}[n] > \tau_{max}[n]) \quad \forall n \in \{1, \dots, N\}$
 $\text{cond2} = \exists(\mathbf{pv}[n] > \tau_{lim}) \quad \forall n \in \{1, \dots, N\}$
 if $\text{cond1} | \text{cond2}$ **then**
 $x_i = x_{i-1} - \frac{x_{i-1}}{k}$
 else
 $x_i = x_{i-1} + \frac{x_{i-1}}{k}$
 $k \leftarrow 2k$
 end if
 $i \leftarrow i + 1$
end while
 $\tau_n = \mathbf{pv}[n] \quad \forall n \in \{1, \dots, N\}$
 $\sqrt{M}_n = \tau_n \mathbf{Q}[n] \quad \forall n \in \{1, \dots, N\}$

$$d_{max}^{(M)} = \frac{\lambda}{4\pi} \left(\frac{P_{tmax}^m G_t^2 G_r^2 M}{S_r} \right)^{1/4} \quad (43)$$

The resulting read range is defined as

$$d_{max}^{(\tau, M)} = \min(d_{max}^{(\tau)}, d_{max}^{(M)}) \quad (44)$$

The condition $d_{max}^{(\tau)} = d_{max}^{(M)}$ yields the condition on the Q factor necessary to achieve the best performance.

$$Q_{max}^{th} = \frac{\sqrt{S_r P_t^{max}}}{S_c} \quad (45)$$

Therefore, by taking into account this condition and by considering the maximum values of τ and M (derived from equations (33) and (34)) at the calculated Q_{max}^{th} , we determine the maximum read range for a tag with chip sensitivity S_c and a reader with read sensitivity S_r as follows:

$$\max_{\tau, M} d_{max}^{(\tau, M)} = \frac{\lambda}{4\pi} \sqrt{G_t G_r \frac{S_c}{2S_r} \left(\sqrt{1 + \frac{4S_r P_t^{max}}{S_c^2}} - 1 \right)} \quad (46)$$

III. UHF RFID TAGS EVALUATION USING THE PROPOSED CHART

In order to illustrate how the proposed chart can be used, we take the chip and antenna pairs presented in the paper [11]. Since the impedances of these chips and antennas are given, the τ and \sqrt{M} can be calculated using (6) and (11). Table I contains the calculated values of τ and \sqrt{M} for all combinations of known chips and antennas, as well as the Q values derived from these two quantities. The values of this table are presented in Fig. 3 by a colored dot with different shapes. Each color refers to a specific antenna (5

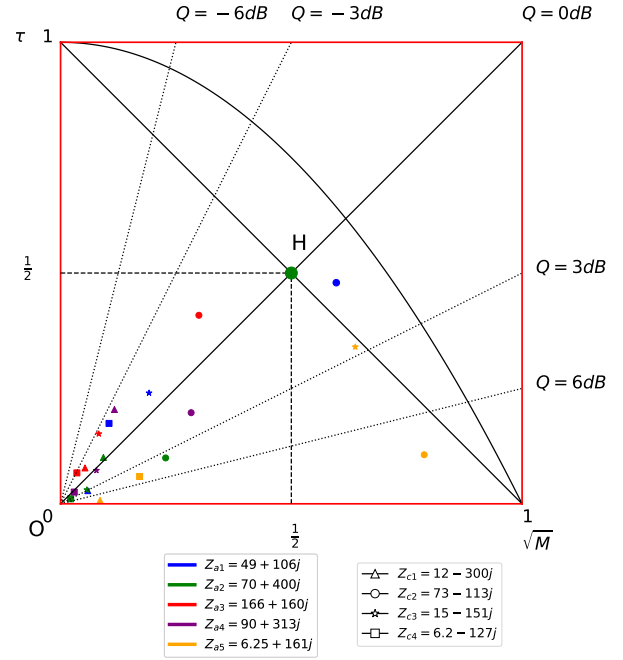


Fig. 3: (\sqrt{M}, τ) chart representation of Bolomey's data

in total) while each shape refers to one specific chip (4 in total). By combining each chip with each antenna, a total of 20 combinations are obtained and presented in the chart.

Since this data are based on the assumption that $Z_1 = 0$, the way to evaluate the performance of the design is assumed to be the distance from the point H which represents a perfect conjugate matching as explained in II-G. Therefore, the criteria to be used for this evaluation is $\rho_{\frac{1}{2}}$ defined in (36). Fig. 4 represents the values of $\rho_{\frac{1}{2}}$ for each combination in an ascending order. As it appears, the combination of chip $Z_{c2} = 73 - 113j\Omega$ and antenna $Z_{a1} = 49 + 106j\Omega$ represented by a blue circle has the highest $\rho_{\frac{1}{2}}$ value among the tags. This combination is the closest to the center (large green circle) with $\tau = 0.479$ and $\sqrt{M} = 0.597$, making it the best design among the tags which balance power absorption and power backscattering. This outcome was expected, as the combination of the two impedances is almost conjugate-matched. On the other hand, it is noticeable that not any combination are effective. In this association procedure many combinations result in very low τ and \sqrt{M} value, thus a very low $\rho_{\frac{1}{2}}$ values such i.e Z_{c4}/Z_{a2} and Z_{c4}/Z_{a4} .

IV. EXPERIMENTAL ASPECTS

A. Experimental Setup

An RFID platform has been used to conduct experiments on UHF RFID tags. The experimental setup shown in Fig. 5 is placed in a $6 \times 4 \times 2.7m^3$ room in the basement of the lab. The platform includes four antennas, 3 of them can move on a portal : one on the top, one on the left one, one on the right side and one antenna is fixed at the extremity of the main rail of the platform. An Alien reader 9900+ is connected to the 4 antennas. The tag support can be translated and rotated, while only the translation has been exploited in these experiments.

| Antenna Impedances | chip impedances | | | | | | | | | | | | | | | |
|--------------------|-----------------|------------|--------|----------|---------|------------|-------|----------|---------|------------|-------|----------|----------|------------|-------|----------|
| | 12-300j | | | | 73-113j | | | | 15-151j | | | | 6.2-127j | | | |
| | τ | \sqrt{M} | Q | Q_{dB} | τ | \sqrt{M} | Q | Q_{dB} | τ | \sqrt{M} | Q | Q_{dB} | τ | \sqrt{M} | Q | Q_{dB} |
| 49+106j | 0.028 | 0.059 | 2.075 | 3.17 | 0.479 | 0.597 | 1.246 | 0.955 | 0.240 | 0.191 | 0.798 | -0.979 | 0.174 | 0.105 | 0.602 | -2.204 |
| 70+400j | 0.100 | 0.092 | 0.923 | -0.347 | 0.099 | 0.227 | 2.290 | 3.598 | 0.030 | 0.057 | 1.879 | 2.739 | 0.010 | 0.022 | 2.024 | 3.062 |
| 166+160j | 0.077 | 0.052 | 0.682 | -1.662 | 0.408 | 0.299 | 0.733 | -1.348 | 0.151 | 0.082 | 0.545 | -2.636 | 0.066 | 0.035 | 0.528 | -2.773 |
| 90+313j | 0.204 | 0.116 | 0.571 | -2.433 | 0.197 | 0.282 | 1.433 | 1.562 | 0.072 | 0.077 | 1.072 | 0.301 | 0.025 | 0.029 | 1.163 | 0.655 |
| 6.25+161j | 0.007 | 0.085 | 11.215 | 10.497 | 0.106 | 0.787 | 7.412 | 8.699 | 0.339 | 0.638 | 1.878 | 2.736 | 0.059 | 0.171 | 2.896 | 4.617 |

TABLE I: τ and \sqrt{M} for a set of known RFID Antennas and IC Chips [11]

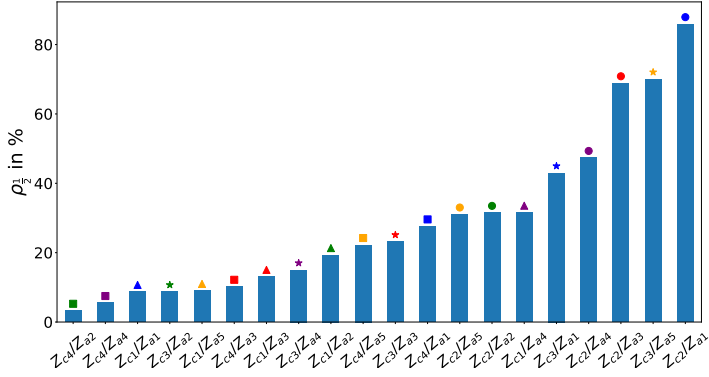


Fig. 4: Ordering the combinations of antenna/tag basing on the $\rho_{\frac{1}{2}}$ performance criteria

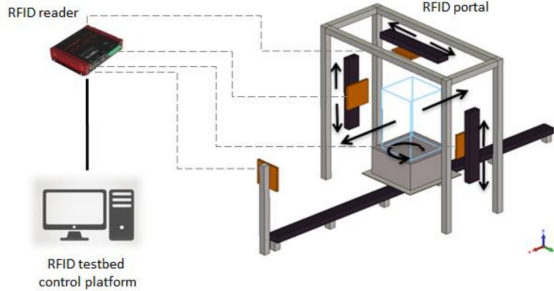


Fig. 5: 5 axes RFID platform (4 translations, 1 rotation) connected to an Alien 9900+ Reader

Fig. 6 represents this translation in a (X,Z) plane where the tag is placed at the same height as the front antenna.

The range of transmitted power goes from 15.7 dBm to 30.5 dBm with a step of 0.1 dBm. The tag is translated on the central rail from a distance between tag and antenna of 0.25 m to 4.83 m over a full range of $R_{max} = 4.58$ m. The selected channel is centred on 866.3 MHz.

A set of tags has been selected in order to compare their performances according to the previously explained characterization theory. Table II displays the features of the selected tags, including their size in mm², chip type, chip sensitivity S_c , calculated tag receptivity R_t using (31) and calculated Q^{th} using (32). All tags are planar and placed in the horizontal support. The photos taken from above, give the indication on the tag orientation w.r.t the antenna. Some of the tags have the same IC chip but different antennas. The tag sensitivity is

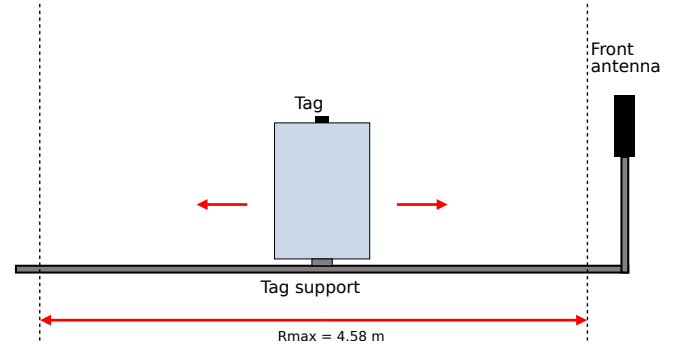


Fig. 6: The translation of the tag support along the main rail represented in plane (X,Z)

calculated, while the typical chip sensitivity is obtained from the chip datasheets. The determination of R_t and Q^{th} from power profiles is presented in the next section.

| Geometry | Tag Name | Size (mm ²) | Chip Name | S_c (dBm) | R_t^{th} (dBm) | Q^{th} (dB) |
|----------|----------|-------------------------|------------|-------------|------------------|---------------|
| | Dogbone | 86 x 24 | Monza 4 | -17.4 | -18.2 | -0.8 |
| | H47 | 44 x 44 | Monza 4 | -17.4 | -19.59 | -2.19 |
| | UPMWEB | 30 x 49 | Monza 4 | -17.4 | -18.73 | -1.33 |
| | AD550 | 41 x 79 | Monza 5 | -17.8 | -19.76 | -1.96 |
| | AD318 | 41.4 x 16 | Monza 5 | -17.8 | -22.45 | -4.65 |
| | AD233 | 70 x 14.5 | Monza 5 | -17.8 | -22.66 | -4.86 |
| | Alien | 94.8 x 8.1 | Higgs 3 | -18 | -20.46 | -2.46 |
| | AD806 | 16 x 16 | NXP Ucode7 | -21 | -19.02 | 1.98 |
| | AD661 | 90 x 19 | Monza R6 | -22.1 | -22.11 | -0.01 |

TABLE II: Characteristics of a collection of commercial tags

B. Measured Power Profiles

For each tag position along the rail, the transmitted power has been swept over the defined range, resulting in $P_{r,dB}(P_t, d)$ which has been obtained by converting the Alien RSSI, at each distance d and for each transmitted power P_t , into a real power quantity in dBm using the conversion formula proposed in [16].

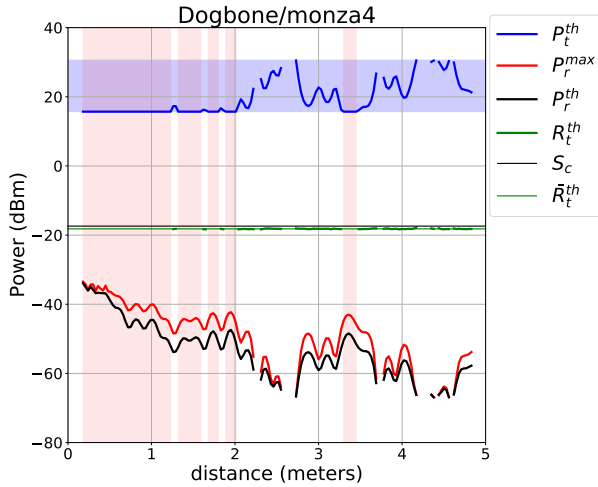


Fig. 7: Power Profiles and Sensitivities Representation

Three power profiles have been defined :

- The transmitted activation profile $P_{t_{dB}}^{th}(d)$ defined in (21). This profile is roughly an increasing function of distance.
- The received activation profile $P_{r_{dB}}^{th}(d)$ defined in (24). This profile is roughly a decreasing function of distance.
- The received power at maximum transmitted power $P_{r_{dB}}^{max}(P_t = P_t^{max}, d)$. This profile is roughly a decreasing function of distance.

Fig. 7 presents the acquisition of these power profiles for the Monza 4 Dogbone tag, the first tag listed in Table II. The Dogbone's chip sensitivity, $S_c = -17.4dBm$, is represented by an horizontal thin black line. The blue line corresponds to the activation profile and is lying in the shaded blue region between the minimum ($P_t^{min} = 15.7dBm$) and maximum ($P_t^{max} = 30.5dBm$) transmitted power from the Alien 9900+ reader. The red line corresponds to the received power profile at the maximum transmitted power ($P_t^{max} = 30.5dBm$). The black thick line represents the received activation profile, obtained from the tag responding at the threshold power. It appears to exhibit a mirroring variation with the transmitted activation profile, due to the reciprocity of the channel. Hence, the tag receptivity R_t^{th} represented by a thick green line, is derived from these two activation profiles, and calculated at each distance using the equation (31). A nearly perfect horizontal line is obtained using this formula, as the effect of the fading channel has been nearly compensated by combining the two profiles. This compensation is grounded in the principle of channel reciprocity, leading to an evaluation of the tag sensitivity, which is independent from the distance and which depends solely on the tag's design. As a result, the mean of tag receptivity (\bar{R}_t^{th}) can be calculated and is represented by an horizontal thin green line. The shift between the mean tag receptivity and the chip sensitivity is given by Q^{th} .

The red region represents the zone where the transmitted and received activation profiles cannot be obtained since it is not possible with the Alien reader to go below the minimum transmission power of $P_t^{min} = 15.7dBm$. It is important to note that, in this region, the received power activation profile

in black is also obtained from the transmission power of $P_t^{min} = 15.7dBm$, and not from the actual activation power of the tag (which is lower than $15.7dBm$). Thus, the blue plot in this region is constant at P_t^{min} and the black plot corresponds to the received power at P_t^{min} . For that reason, the tag receptivity is only evaluated in the complementary region, where the actual activation power is available.

We observe an interruption of the tag response at specific range values, particularly between 2 and 3 meters. This is because even with the maximum transmitted power P_t^{max} , the tag fails to activate, which results from the strong fading in this area.

C. Comparison of Tags Using the Power-Distance Profiles

The same experiment was conducted on the 9 tags under the same conditions to obtain comparable profiles. In Fig. 8, the profile acquisitions for different tags are shown. The first and second rows display sets of Monza 4 and Monza 5 tags, respectively, with different antennas. The third row shows tags with different chips and antennas. For each tag, a subplot presents the 3 profiles and the 3 sensitivities introduced before presented with the same color conventions.

For all the tags measured we find again an almost perfectly horizontal behavior (in green) of the tag receptivity which yield a high reliability to the Q_{dB}^{th} value reported in the table II. The juxtaposition of these 6 graphs illustrates that the difference between the two sensitivities chip and tag varies significantly from one tag to another because of the different designs, even if the chip is the same (i.e. Monza 4 with the 3 observed values of $Q^{th} : -0.8dB, -2.19dB, -1.33dB$).

When looking at the last row of the figure from left to right comes first the Alien tag which seems to be the best since it has the fewest non-detection gaps, then the AD661 which has an almost equal value for chip sensitivity and tag receptivity ($Q^{th} = -0.01dB$), then comes the tag with the clearly worst performance the AD806 with chip NXP Ucode 7 (right bottom). Its read range is 1 meter only, despite having a good chip sensitivity ($S_c = -21dBm$) compared to the other tags. The reason of this behaviour is that this tag has a very small antenna as shown in table II. In addition, it is designed to work on a dielectric surface (such as liquid-filled glass) and not in the air [17].

D. Distribution of the Tag Receptivity Error ϵ_{R_t}

In the following we focus on the estimation error that may appear on the values of Q_{dB}^{th} in equation (32). This is mostly due to the variability of the measured values of R_t^{th} . Fig. 9 shows the distribution of the error

$$\epsilon_{R_t} = R_t^{th} - \bar{R}_t^{th} \quad (47)$$

obtained by aggregating the data from the 9 measured tags (973 points). The error distribution has a rather symmetric shape with an interquartile value of 0.156dBm where most of values of error lie between quartile $Q_1 = -0.08dB$ and $Q_3 = -0.071dB$. The outliers observed do not affect significantly the estimation of R_t^{th} by its mean \bar{R}_t^{th} . We observe that the proposed method has a good accuracy which comes from its exploitation of the channel reciprocity.

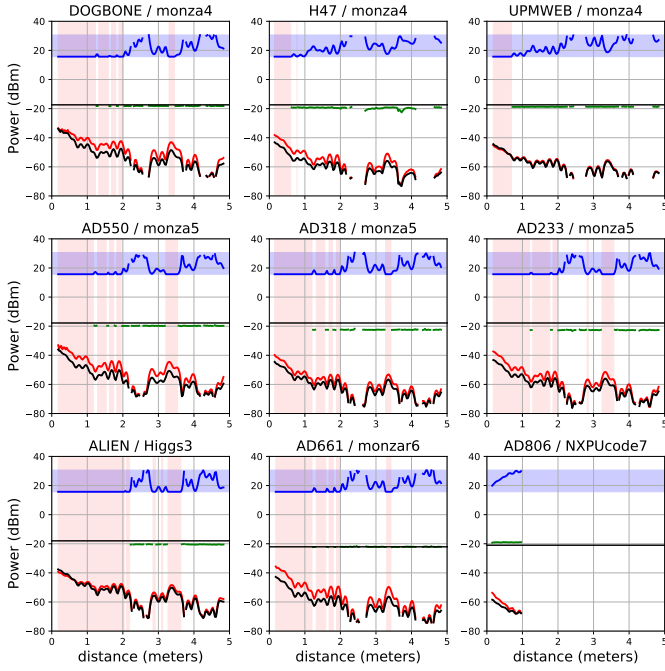


Fig. 8: Power profile diagram for 9 different tags : in red $P_r^{max}(d)$, in black $P_r^{th}(d)$, in blue $P_t^{th}(d)$, in green R_t^{th}

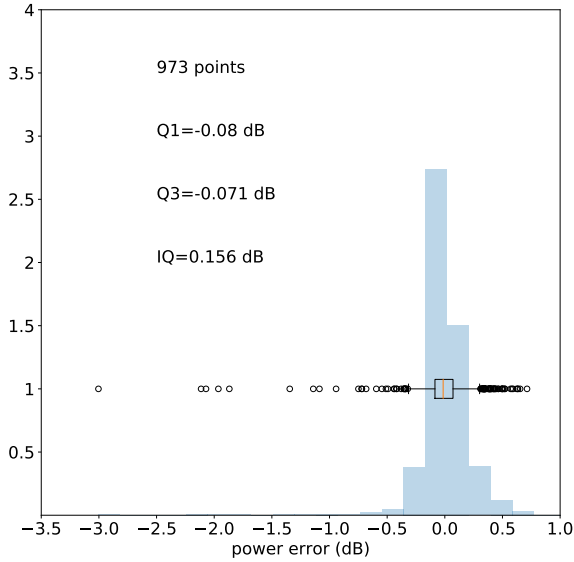


Fig. 9: Distribution of the sensitivity error resolution ϵ_{R_t} obtained for the 9 measured tag profiles

E. Placing the 9 Tags in the Chart using the Interval Halving Algorithm

The Q^{th} values are obtained for the 9 tags using equation (32) and gathered in vector \mathbf{Q} , defined in (40). Additionally, the sequence of ratios \mathbf{t} , defined in (41), is obtained by calculating the ratio between the activation profiles of each

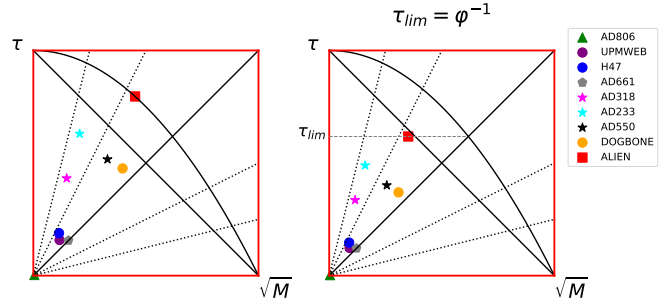


Fig. 10: Proposed chart on a set of tags. On the left: One condition (cond1) applied on the boundary ($\tau = 1 - M$). On the right: Two conditions applied, cond1 and an arbitrary limitation on the value of τ , here $\tau_{lim} = \varphi^{-1}$

sequential pair of tags. This is legitimate because the tags were measured in the same position and channel (see II-H). Using \mathbf{Q} and \mathbf{t} , the algorithm (1) described in II-I is used to obtain the values (τ, M) . Once $(\tau$ and $M)$ are obtained, the tags can be placed in the chart and their relative performances can be compared.

The results in Fig. 10 presents two charts obtained with two different constraints. The first chart on the left enforces that the tag cannot be placed in the impossible zone (only cond1 is applied in algorithm 1). The second chart on the right assumes, in addition, that τ cannot go over τ_{lim} (cond1 and cond2 are applied in algorithm 1). In this case, $\tau_{lim} = \varphi^{-1}$. This limitation is chosen heuristically as it may be unrealistic to assume a design with a higher τ value, as it is the case for the ALIEN tag (red square) in the first chart (left). It is unclear, what is the best possible choice for τ_{lim} in order to access to the more realistic value of τ and M . The ordering of the tags in terms of both τ and M quantities, remains unchanged in both charts, however, the placement of the tags has shifted downwards when adding the limitation on τ in the second chart, while maintaining the same \mathbf{Q} and \mathbf{t} .

F. Evaluation of Tag Performance and Read Range

We define r_{min} as the minimum range where the tag is not responding and r_{max} as the maximum (observed) range where the tag is responding. In addition, we define R as the length (in meters) of the union of tag-responding intervals (i.e the range regions along the rail where the tag is responding). We have $R \leq R_{max}$ (see IV-A), the higher the value of R , the better the tag's performance. Therefore, we define the read range percentage as

$$\rho_{RR} = \left(\frac{R}{R_{max}} \right) \times 100\% \quad (48)$$

Table III presents the results obtained from the 9 tags. It contains two types of parameters: The first type of parameters, including r_{min} , d_{max} , and ρ_{RR} , were directly obtained from the profiles presented in Fig. 8. The second type of parameters, including τ , \sqrt{M} , $\rho_{\varphi^{-1}}$, and $\rho_{\frac{1}{2}}$, were obtained from the chart displayed in Fig. 10. Noting that τ and \sqrt{M} were calculated under the condition $\tau_{lim} = \varphi^{-1}$.

| name | \sqrt{M} | τ | $\rho_{\varphi^{-1}}$ | $\rho_{\frac{1}{2}}$ | ρ_{RR} | r_{min} | r_{max} |
|---------|------------|--------|-----------------------|----------------------|-------------|-----------|-----------|
| AD806 | 0.004 | 0.002 | 0.48 | 0.59 | 19.9 | 0.96 | 0.96 |
| UPMWEB | 0.09 | 0.123 | 17.22 | 21.27 | 75.2 | 2.25 | 4.83 |
| H47 | 0.089 | 0.147 | 18.91 | 23.32 | 78.3 | 2.16 | 4.83 |
| AD661 | 0.121 | 0.121 | 19.61 | 24.24 | 85.7 | 2.22 | 4.83 |
| AD318 | 0.115 | 0.336 | 34.02 | 40.82 | 87.6 | 2.22 | 4.83 |
| AD233 | 0.16 | 0.49 | 45.55 | 51.86 | 92.5 | 2.19 | 4.83 |
| AD550 | 0.256 | 0.401 | 51.7 | 62.74 | 91.9 | 2.16 | 4.83 |
| DOGBONE | 0.308 | 0.37 | 54.55 | 67.18 | 86.3 | 2.22 | 4.83 |
| ALIEN | 0.351 | 0.618 | 69.45 | 73.12 | 95.7 | 2.25 | 4.83 |

TABLE III: Data obtained from tag acquisitions

Tags in this table were sorted in ascending order by the values of $\rho_{\varphi^{-1}}$ calculated by (35). It is difficult to compare the tags based only on their ρ_{RR} , r_{min} and r_{max} values because, except for the AD806, all tags have reached the highest achievable read range of $r_{max} = 4.83m$, thus the maximal detection distance of these tags is unknown. Moreover, the values of ρ_{RR} are close to each other, making it difficult to compare the tags. Consequently, ρ_{RR} , r_{min} and r_{max} are not convenient for comparing the tags.

Fig. 11 presents the values of $\rho_{\varphi^{-1}}$, $\rho_{\frac{1}{2}}$, and ρ_{RR} of the tags depicted in ascending order based on $\rho_{\varphi^{-1}}$ and $\rho_{\frac{1}{2}}$, both of which provide the same performance ordering of the tags. Notice that the ρ_{RR} values shown in green vary slightly from one tag to another whereas $\rho_{\varphi^{-1}}$ and $\rho_{\frac{1}{2}}$ vary more significantly which provide a more sensitive performance ordering. Hence, the tags are ordered from worst to best performance using $\rho_{\varphi^{-1}}$ (or equivalently, in this case, using $\rho_{\frac{1}{2}}$).

Fig. 12 shows the theoretical read range for each tag assuming free space, based on their M and τ values and calculated using formula (44), under the condition $\tau_{lim} = \varphi^{-1}$. The read range is calculated by assuming three different reader sensitivity S_r : $-80dBm$, $-70dBm$ and $-60dBm$, where $S_r = -80dBm$ is the reader sensitivity employed in the current measurements. The figure distinguishes between two types of read range: one is constrained by the forward link ($d_{max}^{(\tau,M)} = d_{max}^{(\tau)}$, represented by no cross-hatched bars), and the other is constrained by the backward link ($d_{max}^{(\tau,M)} = d_{max}^{(M)}$, represented by cross-hatched bars). At $S_r = -80dBm$ the read ranges (in blue) for all the tags are only determined by $d_{max}^{(\tau)}$. This means that the backward link does not have any impact on the read range of these tags at this relatively low reader sensitivity, and the limitation is only due to the forward link. Additionally, the arrangement of the tags based on the calculated read range is similar to the arrangement based on the read range ratio ρ_{RR} obtained from the acquisitions (depicted in blue in Fig. 12). This demonstrates an agreement between the experimental acquisitions and the calculated read ranges. Moreover, we present in Fig. 13 the distribution of τ and M values (given in table III) for the tags with respect to the same order. We observed that the arrangement of the tags based on τ is similar to the arrangement based on the read range ratio ρ_{RR} and the maximum read range d_{max} (except for AD661 which has the best chip sensitivity), validating that the performance of the tags are reflected by their absorption capability in this particular experiment.

However, when imposing a higher S_r value, a limitation

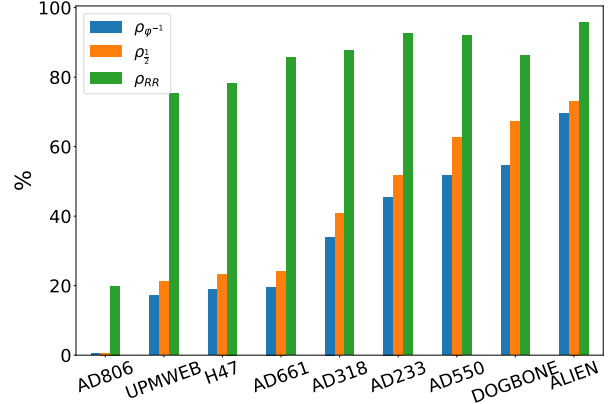


Fig. 11: Comparison of the performance evaluation criterias ($\rho_{\varphi^{-1}}$, $\rho_{\frac{1}{2}}$ and ρ_{RR}) for a set of tags

by the backward link can occurs. When $S_r = -70dBm$ (in red), some tags (AD806, UPMWEB, H47, AD550 and Dogbone) still have read ranges limited by the forward link and remain unchanged, while for other tags (AD661, AD318, AD233 and ALIEN), the backward link becomes the limiting factor, causing a decrease in their read ranges. Consequently, the ranking of the tags in terms of read range is altered. At $S_r = -60dBm$ (in green), the read ranges for all tags are limited by the backward link $d_{max}^{(M)}$. This causes another change in the ordering of the tags by their read range.

Therefore, the arrangement of tags in terms of performance is not definitive as it depends on various factors such as the reader and the application. To address this, the criteria $\rho_{\varphi^{-1}}$ and $\rho_{\frac{1}{2}}$ were suggested as compromised measures to evaluate tag design, striking a balance between τ and M for a design that generally performs well across various scenarios and applications. Further analysis is necessary to determine the optimal method for evaluating tag performance using this methodology.

V. CONCLUSION

This article relates measurable quantities to the well established RFID theory by emphasizing the relationship between the power absorption coefficient and the modulation factor. These two main factors were used to determine the tag sensitivity, and a (\sqrt{M}, τ) chart was proposed to present in a synthetic manner the tag's performance. An RFID characterization platform based on an Alien 9900+ reader is used to measure different distance profiles. The transmitted and received activation profiles specifically were exploited to extract the intrinsic characteristics (τ , M and R_t) of 9 commercial RFID tags measured under the same conditions. Tags are placed in the chart for performance evaluation purpose. To further calculate the free space read range of UHF RFID tags, we used a formula including the two constraints from forward and backward link. A good agreement of this expression is observed for ordering tags by their relative performance.

One key point of the presented work which proposes a thorough over-the-air characterization method is that it can

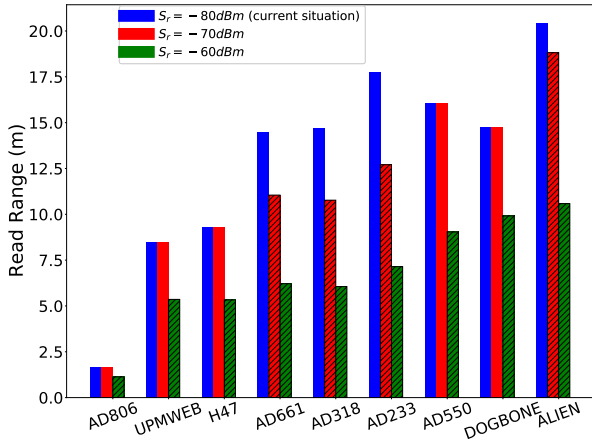


Fig. 12: Theoretical free space read range for different S_r ($G_t = 2\text{dB}$, $G_r = 9\text{dB}$, $P_t^{max} = 30.5\text{dBm}$). Cross-hatched: Backward link-limited, No cross-hatched: Forward link-limited

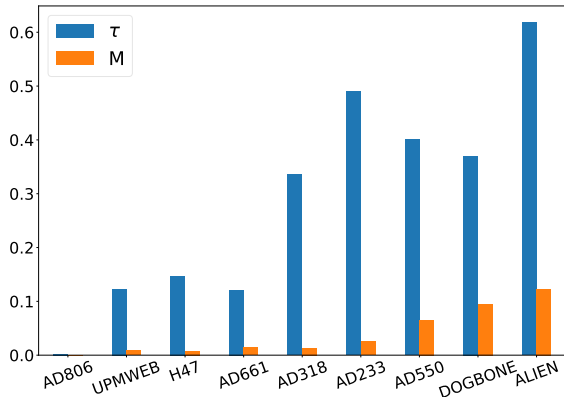


Fig. 13: Distribution of τ and M derived under the condition $\tau_{lim} = \varphi^{-1}$

be implemented in any kind of propagation environment. The method reveals the fundamental and complementary roles played by the mean power transmission coefficient and the modulation factor. This method can be used to evaluate the tag design from both the absorption and backscatter perspectives, providing a practical and simple method for RFID tag characterization.

ACKNOWLEDGEMENT

The authors would like to acknowledge the support of the French BPI project "CAA-Connect" for providing research funding for this project. Their contributions have been instrumental in enabling us to conduct this research.

REFERENCES

[1] D. Dobkin, *The RF in RFID: Passive UHF RFID in Practice*. Newline, 2008.

[2] E. Perret, *Radio Frequency Identification and Sensors*. ISTE Ltd, 2014.

[3] A. de Souza, T. Vuong, Y. Duroc, and A. Luce, "Normalized power calculation to uhf rfid passive tags characterization," in *2014 IEEE Brasil RFID*, 2014, pp. 54–56.

[4] J.-w. Lee, H. Kwon, and B. Lee, "Design consideration of uhf rfid tag for increased reading range," in *2006 IEEE MTT-S International Microwave Symposium Digest*, 2006, pp. 1588–1591.

[5] M. Félix, F. Pereira, V. Ferro, E. Martins, and I. Diniz, "Using labview to automate rfid tag tests: comparison between implemented system and voyantic test system," in *2015 IEEE Brasil RFID*, 2015, pp. 1–5.

[6] L. Catarinucci, D. De Donno, R. Colella, F. Ricciato, and L. Tarricone, "A cost-effective sdr platform for performance characterization of rfid tags," *IEEE Transactions on Instrumentation and Measurement*, vol. 61, no. 4, pp. 903–911, 2012.

[7] R. Colella, L. Catarinucci, P. Coppola, and L. Tarricone, "Characterization system for radiation pattern and sensitivity estimation of uhf rfid tags," in *2015 IEEE International Symposium on Antennas and Propagation USNC/URSI National Radio Science Meeting*, 2015, pp. 1754–1755.

[8] —, "Cost-effective electromagnetic characterization system for radiation pattern and sensitivity estimation of uhf rfid tags," in *2015 IEEE 15th Mediterranean Microwave Symposium (MMS)*, 2015, pp. 1–4.

[9] R. Colella and L. Catarinucci, "Reduction of power-discretization effects in uhf rfid tag performance estimation systems based on off-the-shelf programmable readers," in *2018 3rd International Conference on Smart and Sustainable Technologies (SpliTech)*, 2018, pp. 1–5.

[10] R. Colella, F. P. Chietera, and L. Catarinucci, "Considerations on rigorous uhf rfid tag electromagnetic performance evaluation in non-anechoic environments," in *2020 International Workshop on Antenna Technology (iWAT)*, 2020, pp. 1–3.

[11] J. C. Bolomey, S. Capdevila, L. Jofre, and J. Romeu, "Electromagnetic Modeling of RFID-Modulated Scattering Mechanism. Application to Tag Performance Evaluation," *Proceedings of the IEEE*, vol. 98, no. 9, pp. 1555–1569, Sep. 2010.

[12] P. V. Nikitin, K. V. S. Rao, R. Martinez, and S. F. Lam, "Sensitivity and impedance measurements of uhf rfid chips," *IEEE Transactions on Microwave Theory and Techniques*, vol. 57, no. 5, pp. 1297–1302, 2009.

[13] H. Ge, Y. Yao, J. Yu, and X. Chen, "Binary rfid chip impedance measurement for uhf tag antenna design," in *2014 IEEE Antennas and Propagation Society International Symposium (APSURSI)*, 2014, pp. 1682–1683.

[14] J. D. Griffin and G. D. Durgin, "Complete Link Budgets for Backscatter-Radio and RFID Systems," *IEEE Antennas and Propagation Magazine*, vol. 51, no. 2, pp. 11–25, Apr. 2009, conference Name: IEEE Antennas and Propagation Magazine.

[15] N. Barbot, O. Rance, and E. Perret, "Differential rcs of modulated tag," *IEEE Transactions on Antennas and Propagation*, vol. 69, no. 9, pp. 6128–6133, 2021.

[16] H. E. H. Chehade, B. Uguen, and S. Collardey, "Uhf-rfid power distance profiles for analysis of propagation absorbing effect," in *2021 IEEE International Conference on RFID Technology and Applications (RFID-TA)*, 2021, pp. 157–160.

[17] "Ad-806u7 datasheet," 2021, product Datasheet. [Online]. Available: <https://rfid.averydennison.com/content/dam/rfid/en/products/rfid-products/data-sheets/datasheet-AD-806u7.pdf>